Construction and Building Materials 259 (2020) 119699

Contents lists available at ScienceDirect

Construction and Building Materials

journal homepage: www.elsevier.com/locate/conbuildmat

Influence of laboratory aggregate compaction method on the particle packing of stone mastic asphalt

Henrique Manuel Borges Miranda [a,b,1,*], Fátima A. Batista [c,2], Maria de Lurdes Antunes [d,3], José Neves [e,4]

[a] ISEL – Instituto Superior de Engenharia de Lisboa, Instituto Politécnico de Lisboa, Rua Conselheiro Emídio Navarro, n.° 1, 1959-007 Lisboa, Portugal
[b] CITTA – Centro de Investigação do Território, Transportes e Ambiente, Faculdade de Engenharia da Universidade do Porto & Faculdade de Ciências e Tecnologia da Universidade de Coimbra, Rua Dr. Roberto Frias, s/n, 4200-465 Porto, Portugal
[c] Agência Portuguesa do Ambiente, Lisboa, Portugal
[d] Conselho Diretivo do LNEC, Laboratório Nacional de Engenharia Civil, Lisboa, Portugal
[e] CERIS, Departamento de Engenharia Civil, Arquitectura e Georrecursos, Instituto Superior Técnico, Universidade de Lisboa, Lisboa, Portugal

HIGHLIGHTS

- SMA design depends on optimisation of stone-on-stone in coarse aggregate skeleton.
- Optimisation depends on breakage and air voids of compacted & uncompacted particles.
- Aggregate compaction methods influences particle packing of coarse aggregates.
- Proctor and roller compactor methods are more representative of field conditions.

ARTICLE INFO

Article history:
Received 12 November 2019
Received in revised form 29 April 2020
Accepted 24 May 2020

Keywords:
Stone mastic asphalt
Particle packing
Stone–on–stone
Aggregate compaction methods
Air voids in coarse aggregate mixture

ABSTRACT

The type of aggregates and their packing characteristics under compaction are key factors for the design of asphalt mixtures with improved performance, namely, with respect to resistance to permanent deformation. A good example is Stone Mastic Asphalt (SMA), known by its stone–on–stone structure. In the U.S.A., the aggregate particles packing characteristics in a SMA, specially the stone–on–stone effect, are normally assessed using the "manually dry–rodded" method. However, this method may not be representative of field aggregate particle packing conditions, which may compromise the SMA performance. This article presents new findings regarding aggregate laboratory compaction methods to optimise the coarse aggregate structure in a SMA. Particle breakage, bulk density, air voids (compacted & uncompacted skeleton) in the aggregate / coarse aggregate were assessed for existing methods as well as for new methods using existing compactors, but with different procedures and/or specific devices, e.g. Proctor hammer. The assessed methods were: (1) "non–compaction"; (2) "manually dry–rodded" method; (3) established Proctor compaction; (4) modified Proctor compaction (light and heavy compaction) and (5) steel roller compaction. The 2 latter "new methods" aimed at mechanically simulating the dry-rodded method and the effect of field compactors, respectively. The results highlight that the new laboratory compaction methods developed with Proctor and steel roller compactor, provide a particle packing that is more representative of the field conditions, comparatively to other aggregate compaction methods.

1. Introduction

Stone Mastic Asphalt (SMA) exhibits good performance, especially when applied in wearing courses, due to its high resistance to rutting [1,2]. A key factor contributing to its improved performance is attributed to the aggregate quality [3,4] and the structure created by the SMA non–continuous gradation [5,6], which promotes stone–on–stone contact in the large size aggregates. However, to reach a suitable coarse aggregate skeleton, mix design should not rely exclusively on compositional recipes that focus

* Corresponding author at: ISEL – Instituto Superior de Engenharia de Lisboa, Instituto Politécnico de Lisboa, Rua Conselheiro Emídio Navarro, n.° 1, 1959-007 Lisboa, Portugal.

E-mail addresses: henrique.miranda@isel.pt (H.M.B. Miranda), falexandrab@gmail.com (F.A. Batista), mlantunes@lnec.pt (M. de Lurdes Antunes), jose.manuel.neves@tecnico.ulisboa.pt (J. Neves).

1 https://orcid.org/0000-0003-4062-1402
2 https://orcid.org/0000-0001-7563-8744
3 https://orcid.org/0000-0002-1911-517X
4 https://orcid.org/0000-0002-7131-796

https://doi.org/10.1016/j.conbuildmat.2020.119699
0950-0618/

on achieving a volume of mastic (remaining constituents) that is lower than the air void volume within the coarse aggregates [7].

In order to achieve this goal, several aggregate compaction procedures have been developed and assessed by the scientific community, namely those using the following compactors: dry–rodded compactor [8–10]; Marshall/impact compactor [8,11] and; gyratory compactor [8,11–16]. These methods ordinarily intend to determine the fine/coarse aggregate content to be used in a SMA, minimizing particle aggregate breakage on the coarse aggregate structure (stone–on–stone), which may not, however, be representative of what is obtained in the field.

Other authors use different approaches, such as mathematical modelling with dimensional discrete element methods [17,18,19].

Despite the approach used, in a first stage it is important to choose a suitable compaction method or calibrated model to determine the air voids created by coarser aggregates (normally defined as aggregates with size equal or higher than a "breakpoint" reference sieve).

Nowadays, in the U.S.A. the design of SMA (AASHTO M325) requires the evaluation of the air void content in the coarse aggregates (VCA-DRC) compacted with the dry-rodded compactor (AASHTO T19 and ASTM C29). In this method, coarse aggregates are the ones retained in a given breakpoint sieve (defined according to nominal maximum aggregate size of the asphalt mixture, D). This aggregate compaction is also recommended by other volumetric mix design methods, such as the Bailey method [10]. Despite the dry–rodded compaction being easy to perform and inexpensive, it has, however, two main handicaps: (i) manual compaction is used, which may compromise repeatability and reproducibility between tests performed by different technicians or labs; and (ii) it uses low compaction energy, which may not be representative of what occurs in the field (particle packing and breakage), as reported by Brown and Haddock (1997) [8]. Thus, lower compaction energy typically promotes the design of SMA with higher content of fine aggregates (passive particles), rather than coarse aggregates (active particles). This results in SMA with lower resistance to permanent deformation as reported in Austroads (2013) [20].

In this context, a study on alternative aggregate compaction methods that could provide enhanced SMA design was carried out. Besides the established "manually dry–rodded" method, the following laboratory methods for compaction of the coarse aggregates were assessed:

(1) "non-compaction", i.e. the voids characteristics of the loose coarse aggregates inside a container of known volume were considered;
(2) manually dry–rodded method;
(3) Proctor compaction, both applying the original standard effort (light compaction) and applying the modified effort (heavy compaction);
(4) Proctor compaction with modified rammer, simulating the dry-rodded method, but performed mechanically with Proctor compactor (developed within the present study);
(5) compaction of the coarse aggregates using the "steel roller compactor" (which also consisted in a new method, since it is currently used only for asphalt mixtures).

The present paper describes the above-referred study and highlights suitable aggregate compaction methods for laboratory optimisation of the contact between coarse aggregates, used for further design of SMA (asphalt mixture) [21].

This study was validated using diverse aggregate types (e.g. different natures) combined with different preparation and compaction methods. Additionally, samples of two different SMA used in actual road pavements were collected and studied. The validation was also complemented with: (i) the ratio range specified in Bailey method for SMA mix design to achieve stone-on-stone contact between coarse aggregates, as well (ii) the range of air void content (VCA) in the coarse aggregates reported by Nicholls (1998) [22] and Drueschner (2005) [23] to ensure adequate space for mastic after SMA compaction.

This study is part of a broader research regarding the first stage of the development of a new SMA mix design approach [24]. In fact, an adequate framework for SMA mix design should ensure the most suitable stone-on-stone effect between the aggregates in order to minimize particle aggregate breakage and to optimize the mastic volume inside the space provided by coarse aggregates. So, the determination of bulk density and air void content of the coarse aggregates through the most adequate compaction method, representative of field conditions, is essential. The results of the second stage, regarding the design of the asphalt mixtures, can be found elsewhere [21].

2. Materials and research methodology

The laboratory tests were conducted on crushed aggregates commonly used in Portugal: granodiorite (0/4, 6/10 mm), basalt (4/12 mm), and granite (0/5, 6/16 mm).

Furthermore, the granodiorite and basalt aggregates were used for two asphalt mixtures (SMA 12, SMA 14, respectively) that were applied in two actual road pavements in Portugal. Asphalt samples were collected from both pavements after construction and directly from the paver for further study in the laboratory.

Tables 1 and 2 show the physical properties and the gradation of the materials used in this study, respectively. Moreover, for each aggregate fraction in Table 2, different coarse aggregate fractions were sieved, as portions of the total aggregate blends retained in different breakpoint sieves (2 mm, 4 mm and 4.75 mm). The breakpoint sieve (BP) is considered as a boundary sieve for SMA mixtures, from which the coarse skeleton starts, depending on the maximum aggregate size of the asphalt mixture, D [25].

In this study, the breakpoint sieves (Table 3) were defined with reference to the sieve sizes specified for SMA in the European Standard (EN 13108–5) using the ratio between the BP and D (nominal maximum size) recommended for a SMA mixture, both in the method described in AASHTO M325 standard and in the Bailey method. According to Vavrik (2000) [26], the BP/D ratio can range, in a 2D analysis, from 0.16 (no crushed faces) to 0.29 (all crushed faces) and, in a 3D analysis, from 0.15 (hexagonal structure) to 0.42 (cubic structure).

As shown in Table 3, the breakpoint sieves selected for this study have a ratio in relation to D, BP/D, between 0.28 and 0.32, which is within the range obtained by AASTHO M325 and Bailey methods. However, the use of breakpoint sieves with lower mesh dimension (European sieves: 2 mm and 4 mm) compared to AASHTO M325 (American sieves: 2.36 mm and 4.75 mm) will contribute for the design of SMA with lower permeability, as studied by Cooley and Brown (2003) [27]. The use of a breakpoint sieve with dimension equal to 4 mm instead of 4.75 mm, as used in the U.S.A., intends to adapt the breakpoint sieve concept to European conditions.

2.1. Research methodology

The particle packing characteristics to optimise the contact between coarse aggregates, were evaluated according to the experimental programme presented in Table 4 for different compaction methods.

The testing program included the following assessment for aggregates: (i) bulk density of a compacted aggregate structure

Table 1
Aggregate properties.

Test	0/4 mm(Granodiorite)	6/10 mm(Granodiorite)	4/12 mm(Basalt)	0/5 mm(Granite)	6/16 mm(Granite)
Particle shape, FI (%)	-	FI_{10}	FI_{15}	-	FI_{20}
Los Angeles, LA (%)	-	LA_{20}	LA_{15}	-	-
Micro Deval, MDE (%)	-	MDE_{10}	MDE_{10}	-	-
Polished stone value, PSV (%)	-	PSV_{44}	PSV_{50}	-	PSV_{44}
Water absorption, WA_{24} (%)	$WA_{24}1$	$WA_{24}1$	$WA_{24}1$	$WA_{24}1$	$WA_{24}1$
Specific gravity (Mg/m^3)	2.615	2.723	2.968	2.680	2.667

Table 2
Aggregate fractions/asphalt mixture gradations.

Aggregate fraction & mixture	Sieve (mm) / Percentage passing by mass													
	20	16	14	12.5	10	8	6.3	4	2	1	0.500	0.250	0.125	0.063
0/4 mm	-	-	-	-	-	-	-	100	77	46	29	19	13	11.0
6/10 mm	-	-	-	100	80	45	16	4	3	3	3	3	2	1.7
4/12 mm	-	100	98	93	51	22	7	1	1	1	1	1	1	0.6
0/5 mm	-	-	-	-	-	-	100	82	57	39	27	19	13	8.6
6/16 mm	-	100	88	80	56	36	18	5	3	2	2	1	1	0.6
SMA 12	-	-	-	100	87	65	46	38	30	21	16	13	9	7.3
SMA 14	100	99	91	78	59	48	39	27	23	19	16	14	11	8.9

Table 3
Breakpoint sieve.

D, nominal maximum aggregate size (mm)	AASHTO M325		Bailey method		European sieves		Selected breakpoint sieve, BP (mm)
	BP (mm)	Ratio BP/D	BP (mm)	Ratio BP/D	BP (mm)	Ratio BP/D	
14	4.75	0.34	2.36	0.17	2/4/5.6	0.14/0.28/0.40	4
12 (12.5)	4.75	0.38	2.36	0.19	2/4/5.6	0.16/0.32/0.45	4

Notes: D – nominal maximum aggregate size; BP – Breakpoint sieve

Table 4
Experimental programme.

Aggregate laboratory compaction method	Rammer mass(kg)	Number of layers & number of blows per each layer	Aggregate portion	Aggregate type		
				Granodiorite	Basalt	Granite
Non-compaction	–	1 / -	Fraction	■		■
			BP 2 mm	■		
			BP 4 mm	■	■	■
			BP 4.75 mm	■		
Dry-rodded	Manual	3 / 25	Fraction	■		■
			BP 2 mm	■		
				■	■	■
			BP 4 mm	■		
			BP 4.75 mm			
Proctor	2.49	3 / 25	Fraction	■		
			BP 2 mm	■		
			BP 4 mm	■		
				■	■	
			BP 4.75 mm			
	2.49	3 / 50	BP 4 mm	■		
	2.49	3 / 75	BP 4 mm	■		
	4.54	5 / 55	BP 4 mm	■	■	■
Proctor modified rammer	2.49	3 / 25	BP 4 mm	■	■	■
Steel roller (with vibration)	–	1 / 15	Fraction	■		■
			BP 2 mm			
			BP 4 mm	■	■	
			BP 4.75 mm	■		■
				■		

Notes: Fraction – refers to the total aggregate blend (coarse, fine and filler) without any material sieving removal; BP – Breakpoint sieve; BP 2 mm – coarse aggregate portion of the total aggregate blend retained on the sieve with mesh equal to 2 mm; BP 4 mm – coarse aggregate portion of the total aggregate blend retained on the sieve with mesh equal to 4 mm; BP 4.75 mm – coarse aggregate portion of the total aggregate blend retained on the sieve with mesh equal to 4.75 mm.

and its relation with the loose bulk density; (ii) air void content in the uncompacted/compacted aggregates (VCA), and (iii) particle breakage, determined from the increment of particles passing the breakpoint sieve 4 mm due to compaction. Furthermore, the particle breakage was also validated for granodiorite and basalt aggregates further used in field SMA mixtures (SMA 12 and SMA 14, respectively). Validation was determined using aggregates obtained after incineration of asphalt samples collected from pavements after construction (Fig. 1). Particle breakage was calculated from the increment of particles passing the selected breakpoint

Fig. 1. Compacted samples of asphalt mixture collected from the pavement.

Fig. 2. Uncompacted sample of asphalt mixture collected directly from the paver.

sieve (4 mm) comparatively to the initial gradation defined in the mix design.

The same procedure was used for the samples of asphalt mixture (SMA 12) collected directly from the paver, in order to evaluate particle breakage prior to compaction (Fig. 2).

2.2. Aggregate compaction methods

2.2.1. Non-compaction method

The non-compaction method was performed with the procedure per in the European standard EN 1097–3. The samples of aggregate are dried in the oven to a constant mass. The individual samples (three) must be 125% to 150% of the amount that fits in the cylindrical container (diameter of 170 mm; height of 240 mm), for which the volume was previously determined. The container is filled with aggregates till overflowing, after which the excess of aggregates is removed and the surface is levelled off.

For each uncompacted sample, its loose bulk density (ρ_{NC}) was calculated using the equation:

$$\rho_{NC} = \frac{m_2 - m_1}{V} \quad (1)$$

$\rho_{NC}$is the loose bulk density (Mg/m^3);

$m_1$is the mass of the cylindrical container (kg);

$m_2$is the mass of the cylindrical container and uncompacted aggregates/coarse aggregates (kg);

$V$is the internal volume of the cylindrical container (L).

For each uncompacted sample, its air void content in the aggregates/coarse aggregates (VCA_{NC}) was calculated using the equation:

$$VCA_{NC} = \frac{\rho_p - \rho_{NC}}{\rho_p} \cdot 100 \quad (2)$$

$VCA_{NC}$is the air void content in the uncompacted aggregates/-coarse aggregates (%);

$\rho_p$is the aggregate density (Mg/m^3);

$\rho_{NC}$is the loose bulk density (Mg/m^3).

2.2.2. Dry-rodded method

The dry-rodded method was performed by adapting the procedure described in the American standards AASHTO T19 and ASTM C29 to the European standard EN 1097–3, which prescribes aggregate compaction for evaluation of bulk density and air void content in the compacted aggregates, without, however, specifying any procedure.

The main differences between American and European procedures relate to:

- The volume of the cylindrical container: In this study, the volume specified in the European standard of 5 L for nominal maximum aggregate size, D, equal to 16 mm, was used. This volume is always larger than the described in the AASHTO T19 and ASTM C29 (around 4.6 L for D equal to 16 mm), thus leading to more representative samples.
- The dimensions of the cylindrical container: The ratio between the internal diameter of the container and its height should be 0.5 to 0.8, according to the European standard. This requirement is omitted both in AASHTO T19 and in ASTM C29. Therefore, the evaluation was performed using the same cylindrical container (170 mm diameter, 240 mm height) as used in the non-modified method.
- The amount of each aggregate sample (three) should be 125% to 200% of the amount that fits in the container (AASHTO T19 and ASTM C29), comparatively to 120% to 150% (EN 1097–3). In this case, individual samples with 125% to 150% of the amount that fits the container were used.

The aggregate compaction was performed according to the procedure described in the AASHTO T19 and ASTM C29, which requires pouring aggregates in the container and compacting them in three equal layers (Fig. 3). For each layer, 25 blows with the tamping rod were evenly distributed over the surface (avoiding hitting the bottom of the container). After filling the container, the excess of aggregates was removed and the surface was levelled off.

For each dry-rodded compacted sample, the bulk density (ρ_{DRC}) and its air void content (VCA_{DRC}) were calculated according to equations (1) and (2), respectively.

2.2.3. Proctor and Proctor with modified rammer methods

The Proctor compaction was used in this study due to its similarity to the dry-rodded method, as far as concerns to: (i) dimension and volume of the cylindrical moulds (containers), (ii) type of compaction (by impact), (iii) compaction by layers and even distribution of blows over the aggregate surface.

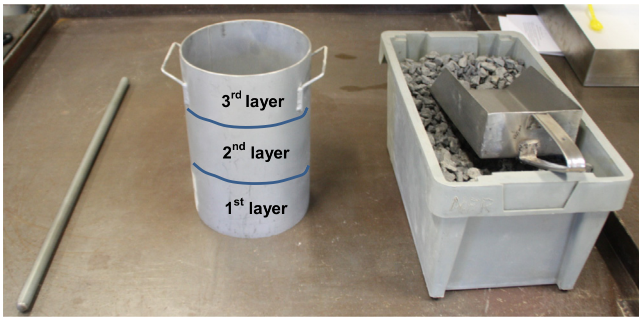

Fig. 3. Dry-rodded apparatus and example of layers to compact.

The main advantage of this method comparatively to the dry–rodded method, is its automated compaction procedure (compaction energy, height of drop, and distribution of blows), contributing for repeatability and reproducibility improvements.

The Proctor compaction was firstly performed by simply adapting the procedure described in the European standard EN 13286–2 to the standards AASHTO T19 and ASTM C29 (related to the "dry–rodded compaction") and also to EN 1097–3.

Thus, to ensure the volume and ratio between the internal diameter of the mould and its height according to the EN 1097–3, the large mould with extension was used. Therefore, the mould (Fig. 4) used in both Proctor methods had the following dimensions: diameter of 150 mm; height of 228 mm.

The aggregate compaction performed requires, similarly to the dry-rodded method, pouring aggregates in the mould (Fig. 4) and compacting them in equal layers. For each layer, different number of blows with the hammer was evenly distributed over the surface. After filling the mould, the excess of aggregates was removed and the surface was levelled off.

In this study changes were performed concerning the mass of the rammer (2.49 kg and 4.54 kg), as well as the number of layers (three and five) and number of blows per layer (25, 50, 75 and 55 blows) as described in Table 4.

Furthermore, a new Proctor rammer was developed in order to simulate the tamping rod action in accordance with the dry-rodding procedure described in AASHTO T19 and ASTM C29. The new Proctor rammer was designed taking into account the compactor equipment characteristics and restrictions. As so, one end is for fixation to the equipment, the other end is rounded in a hemispherical tip, and the rod rammer is 15 mm in diameter and 95 mm height, as shown in Fig. 4.

The aggregate compaction procedure (similar to the dry-rodded method) regards pouring aggregates in the mould and compacting them in three equal layers. For each layer, 25 blows with the modified rammer (mass of the rammer 2.49 kg) were evenly distributed over the surface. After filling the mould with aggregates, excess of aggregates is strike off and levelled off the surface.

For each Proctor and Proctor with modified rammer compacted sample, the bulk density (ρ_{PC}) and its air void content (VCA_{PC}) were calculated using equations (1) and (2), respectively.

2.2.4. Steel roller method

This new steel roller method was used in this study due to its similarity to the compaction methods used in the field. The compaction made with this method is done with rolling loads, instead of using impact loads. Additionally, vibration was used in order to promote easier particle packing.

The steel roller method was performed by adapting the procedure described in the European Standard EN 12697–33 to EN 1097–3. Also, in this case, individual aggregate samples with 125% to 150% of the amount that fits in a square mould (300 mm × 300 mm × 50 mm) were used.

The aggregate compaction was performed according to the following experimental procedure (Fig. 5):

(1) Pour the materials into the corners of the square mould without overflowing it, in order to make further compaction easier and avoid excessive particle breakage.
(2) Fill the rest of the mould without overflowing and even out the material in order to scrape away any excess aggregates or to compensate for any gaps between them.
(3) Apply the rolling load for 15 cycles with vibration.
(4) After first compaction (3) seek for gaps in the surface of the aggregates, especially in the corners. In Fig. 5 the red spots show existing gaps to fill. Level off the surface without overflowing the mould. Repeat the compaction process (3).
(5) Repeat (4) as many times as needed to ensure a full-levelled aggregate surface.

Fig. 4. Mould used and new Proctor rammer developed for tamping rod simulation.

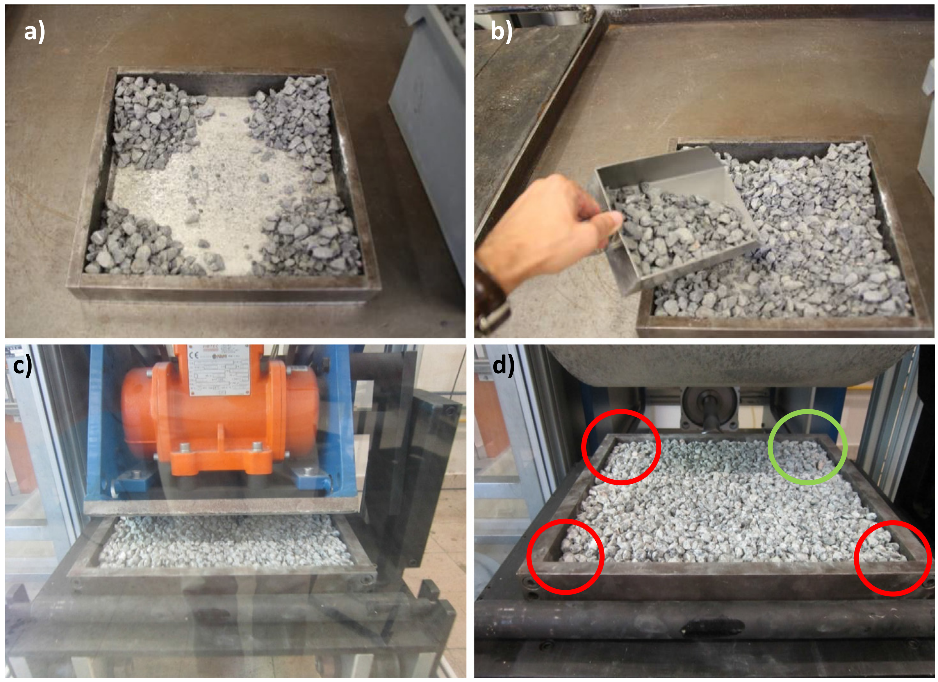

Fig. 5. Aggregate compaction procedure with steel roller compactor.

(6) Compute the mass of the compacted sample by weighting the mould with and without aggregates.

For each steel roller compacted sample, the bulk density (ρ_{RC}) and its air void content (VCA_{RC}) were calculated using the equation (1) and (2), respectively.

3. Results and discussion

The results of aggregates/coarse aggregates bulk density (BD) obtained from each compactor (BDc) and their relation with the loose bulk density of the uncompacted aggregates (BDuc), as well the respective air void content, VCA, were evaluated (Table 5). Furthermore, particle breakage (increment of particles content passing in the breakpoint sieve 4 mm, comparatively to the initial gradation defined in the mix design) for granodiorites and basalts used in the laboratory were compared with field applications (SMA 12 and SMA 14, respectively) and presented in Table 6.

Figs. 6 and 7 present the results for the VCA obtained with different aggregate compaction methods, for individual fractions and for coarse aggregate mixture (sieved portion of the total aggregate blends retained in different breakpoint sieves 2 mm, 4 mm and 4.75 mm). Moreover, the correlation between VCA and the BDc/BDuc (ratio between compacted & uncompacted aggregates bulk densities) is plotted in Fig. 8.

Fig. 6 shows the variation of air void content across the different compaction methods obtained for the granodiorite production coarse aggregate fraction (6/10 mm) and for coarse aggregate mixtures for different breakpoint sieves (2, 4, and 4.75 mm). As expected, the air volume decreases as compaction energy increases. Steel roller and Proctor (55 blows, 5 layers) produce the lowest air voids. However, for each compaction method the air void contents obtained for the complete aggregate fraction (6/10 mm) are similar to the ones obtained for any of the coarse aggregates retained in breakpoint sieves (2 mm, 4 mm and 4.75 mm). According to these results, we can assume that if we choose a coarse aggregate production fraction whose lower dimension (in this case 6 mm) is not under the BP sieve size, there is not much difference in the compactions obtained with each method for the production fraction or for any of the chosen BP coarse aggregates.

The lower dimension of coarse aggregate fraction should be higher than the selected breakpoint sieve (Table 3).

Fig. 7 shows, for coarse aggregates retained in breakpoint sieve 4 mm, the variation of air void content across different compaction methods and aggregate nature. As expected, steel roller and Proctor (55 blows, 5 layers) produce the lowest air voids, since these correspond to higher energy.

For each compaction method, the variation of air void content among aggregates of different natures (granodiorite, basalt and granite) for coarse aggregates retained in breakpoint sieve 4 mm is small, except for steel roller and Proctor (55 blows, 5 layers).

Fig. 8 shows the relation between the air void content and the ratio between compacted/uncompacted aggregates. The Figure also shows: (i) the ratio range of 1.10 (110%) to 1.25 (125%) specified in Bailey method for SMA mix design to achieve stone-on-stone contact between coarse aggregates; (ii) the range of air void content, VCA (35% – 40%) in the coarse aggregates reported by Nicholls (1998) [22] and Drueschner (2005) [23] to ensure adequate space for the mastic after compaction of the SMA, with a porosity of 2.5% to 5.0%.

The results in Fig. 8 put in evidence, as expected, a good correlation (linear regression, R = 92%) between VCA and BDc/BDuc ratio. Air void content increases as that ratio decreases, as a result of lower compaction effort, and therefore, lower bulk density of compacted aggregates.

The dry–rodded method does not comply with the range specified by the Bailey method (1.10 – 1.25), nor achieve the range of 35% – 40 % for VCA, independently of aggregate nature or fraction/coarse aggregates used. Similar results were obtained for the Proctor method (25 blows, 3 layers) and the Proctor modified rammer.

Only samples tested using Proctor compaction (50 / 75 blows × 3 layers; 55 blows × 5 layers) have complied with both ranges previously mentioned.

Table 5
Bulk density (compacted & uncompacted aggregates and respective ratio) and air voids in the aggregates.

Aggregate laboratory compaction method	Aggregate type	Aggregate portion	BDc(Mg/m^3)	BDuc(Mg/m^3)	Ratio BDc/BDuc	VCA(%)
Non-compaction	Granodiorite	0/4 mm	-	1.410	1.00	46.1
		6/10 mm	-	1.461	1.00	46.3
		BP 2 mm	-	1.490	1.00	45.4
		BP 4 mm	-	1.440	1.00	47.1
		BP 4.75 mm	-	1.438	1.00	47.2
	Basalt	BP 4 mm	–	1.578	1.00	47.0
	Granite	0/5 mm	–	1.481	1.00	44.7
		BP 4 mm	-	1.424	1.00	46.6
Dry-rodded[1)]	Granodiorite	0/4 mm	1.540	1.410	1.09	41.1
		6/10 mm	1.550	1.461	1.06	
		BP 2 mm	1.580	1.490	1.06	43.0
		BP 4 mm	1.550	1.440	1.08	41.9
		BP 4.75 mm	1.540	1.438	1.07	43.0
						43.4
	Basalt	BP 4 mm	1.730	1.578	1.09	42.0
	Granite	0/5 mm	1.590	1.481	1.07	40.6
		BP 4 mm	1.520	1.424	1.07	43.1
Proctor[2)]	Granodiorite	0/4 mm	1.700	1.410	1.21	34.8
		6/10 mm	1.540	1.461	1.05	43.4
		BP 2 mm	1.560	1.490	1.05	42.7
		BP 4 mm	1.613	1.440	1.12	40.8
		BP 4.75 mm	1.530	1.438	1.06	43.9
	Basalt	BP 4 mm	1.760	1.578	1.11	40.8
Proctor modified rammer[3)]	Granodiorite	BP 4 mm	1.620	1.440	1.13	40.4
	Basalt	BP 4 mm	1.770	1.578	1.12	40.5
	Granite	BP 4 mm	1.530	1.424	1.08	42.5
Proctor[4)]	Granodiorite	BP 4 mm	1.640	1.440	1.14	39.6
Proctor[5)]	Granodiorite	BP 4 mm	1.660	1.440	1.15	39.1
Proctor[6)]	Granodiorite	BP 4 mm	1.700	1.440	1.18	37.5
	Basalt	BP 4 mm	1.820	1.578	1.15	38.9
	Granite	BP 4 mm	1.700	1.424	1.20	36.3
Steel roller[7)]	Granodiorite	0/4 mm	1.650	1.410	1.17	37.1
		6/10 mm	1.610	1.461	1.10	41.0
		BP 2 mm	1.650	1.490	1.11	39.4
		BP 4 mm	1.740	1.440	1.21	36.1
		BP 4.75 mm	1.700	1.438	1.18	37.4
	Basalt	BP 4 mm	1.770	1.578	1.12	40.5
	Granite	0/5 mm	1.840	1.481	1.24	31.3
		BP 4 mm	1.560	1.424	1.10	41.7

Notes: BP – Breakpoint sieve; BP 2 mm – coarse aggregate portion of the total aggregate blend retained in the sieve with mesh equal to 2 mm; BP 4 mm – coarse aggregate portion of the total aggregate blend retained in the sieve with mesh equal to 4 mm; BP 4.75 mm – coarse aggregate portion of the total aggregate blend retained on the sieve with mesh equal to 4.75 mm; BDc – aggregates/coarse aggregates bulk density obtained from different compaction methods; BDuc – loose bulk density of the uncompacted aggregates; VCA – air void content of uncompacted/compacted aggregates.
[1)] 25 blows for each layer (3 layers).
[2)] 25 blows (2.49 kg) for each layer (3 layers).
[3)] 25 blows with modified rammer (2.49 kg) for each layer (3 layers).
[4)] 50 blows (2.49 kg) for each layer (3 layers).
[5)] 75 blows (2.49 kg) for each layer (3 layers).
[6)] 55 blows (4.54 kg) for each layer (5 layers).
[7)] 15 rolling sequences with vibration.

The linear regression shows that VCA should be between around 33% and 41% (similar to [22,23], to achieve the ratio range (1.10 – 1.25) specified in Bailey method for SMA mix design.

The results presented in Table 6 are plotted in Fig. 9 for further discussion of the correlation between VCA and the particle breakage, expressed as the increment of particles content passing in the breakpoint sieve 4 mm.

Fig. 9 is complemented with: (i) the range of air void content (35% – 40%) in coarse aggregates reported by Nicholls (1998) [22] and Drueschner (2005) [23], and (ii) studies that show a particle breakage increase between 2.5% and 9.0% for the breakpoint sieve 4.75 mm [28,29], on samples collected from the field.

The results in Fig. 9 show a good correlation (linear regression, R^2 = 80%) between air void content and the particle breakage (increment of particles content passing in the breakpoint sieve 4 mm). The particle breakage, ranged from 0.5% (dry–rodded method) to 7.6% (Proctor, 55 blows, 5 layers) and from 2.3% to 4.0% in the samples collected from the two actual road pavements.

Steel roller and Proctor (55 blows, 5 layers) produced the highest particle breakage. These two methods had also obtained the lowest air void contents (Figs. 6 and 7), which were, according to Fig. 9, mainly the results from particle breakage. Similar conclusion was obtained by Brown and Haddock (1997) [8] for other compaction methods. However, in the steel roller method, vibration may have contributed in basalt and granites for a better particle packing reducing particle breakage comparing to Proctor (55 blows, 5 layers).

Fig. 8 shows that the dry–rodded method does not comply with the range (35% – 40%) for the air void content, independently of aggregate nature used or fraction/coarse aggregate fraction used. Similar results were obtained for the Proctor method (25 blows, 3 layers) and the Proctor with modified rammer.

Once again, only samples tested with the three Proctor compaction methods – 50 / 75 blows × 3 layers and 55 blows × 5 layers – have complied within both ranges previously mentioned. From these three methods, and due to the similarity of Proctor procedure

Table 6
Particle breakage for coarse aggregates retained in breakpoint sieve 4 mm.

Aggregate laboratory compaction method	Aggregate type	Breakpoint Sieve	VCA (%)	Particle breakage, increment of particles content passing in breakpoint sieve, 4 mm (%)
Dry-rodded[1)]	Granodiorite	4 mm	43.0	0.5
	Basalt		42.0	0.5
	Granite		43.1	0.5
Proctor[2)]	Granodiorite	4 mm	40.8	0.8
	Basalt		40.8	0.8
Proctor modified rammer[3)]	Granodiorite	4 mm	40.4	1.3
	Basalt		40.5	1.7
	Granite		42.5	2.0
Proctor[4)]	Granodiorite	4 mm	39.6	3.5
Proctor[5)]	Granodiorite	4 mm	39.1	3.8
Proctor[6)]	Granodiorite	4 mm	37.5	4.4
	Basalt		38.9	4.0
	Granite		36.3	7.6
Steel roller[7)]	Granodiorite	4 mm	36.1	6.7
	Basalt		40.5	1.4
	Granite		41.7	3.1
SMA 12[8)]	Granodiorite	4 mm	–	3.2
SMA 12[9)]	Granodiorite	4 mm	–	2.3
SMA 14[9)]	Basalt	4 mm	–	4.0

Notes: VCA – air void content of uncompacted/compacted aggregates.
[1)] 25 blows for each layer (3 layers).
[2)] 25 blows (2.49 kg) for each layer (3 layers).
[3)] 25 blows with modified rammer (2.49 kg) for each layer (3 layers).
[4)] 50 blows (2.49 kg) for each layer (3 layers).
[5)] 75 blows (2.49 kg) for each layer (3 layers).
[6)] 55 blows (4.54 kg) for each layer (5 layers).
[7)] 15 rolling sequences with vibration.
[8)]sample collected directly from the paver.
[9)]samples collected from compacted pavement.

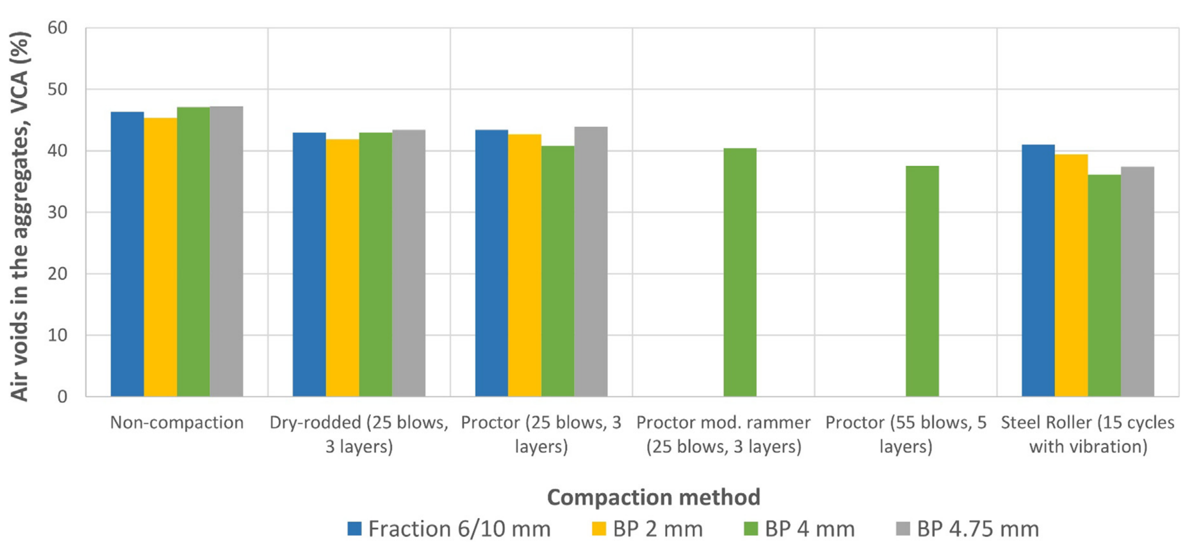

Fig. 6. Air void content for granodiorites for production fraction (6/10 mm) and for coarse aggregate mixtures using different compaction methods.

(55 blows, 5 equal layers) with the specified in the EN 13286–2, this may be seen as a method for further study to optimise coarse particle packing, for a stone-on-stone effect.

4. Conclusions

The results from a research study on the effects of different laboratory aggregate compaction methods on the particle packing of coarse aggregates are presented in this paper. The research highlights new laboratory compaction methods, herein developed, which can provide a particle packing more representative of the field conditions comparatively to other methods traditionally used.

To evaluate the particle packing characteristics that optimises the contact between coarse aggregate particles, different aggregate laboratory compaction methods were used: (1) "non–compaction"; (2) "manually dry-rodded" method; (3) Proctor compaction using the typical rammer; 4) Proctor compaction using a specific developed rammer; and (5) compaction using the steel roller compactor. Comparative result analysis was also made with two SMA collected from road pavements and directly from paver.

The data leads to the following main conclusions:

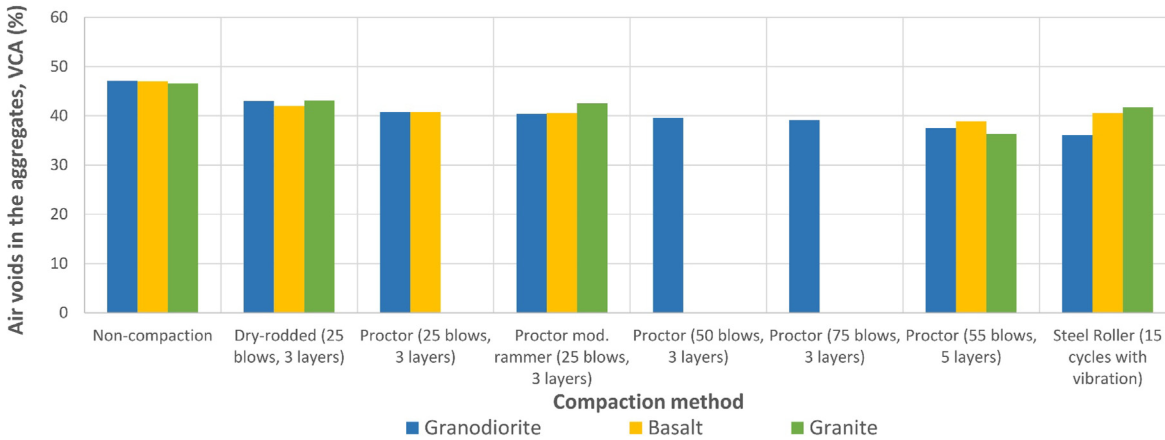

Fig. 7. Air void content by compaction method for breakpoint sieve (4 mm).

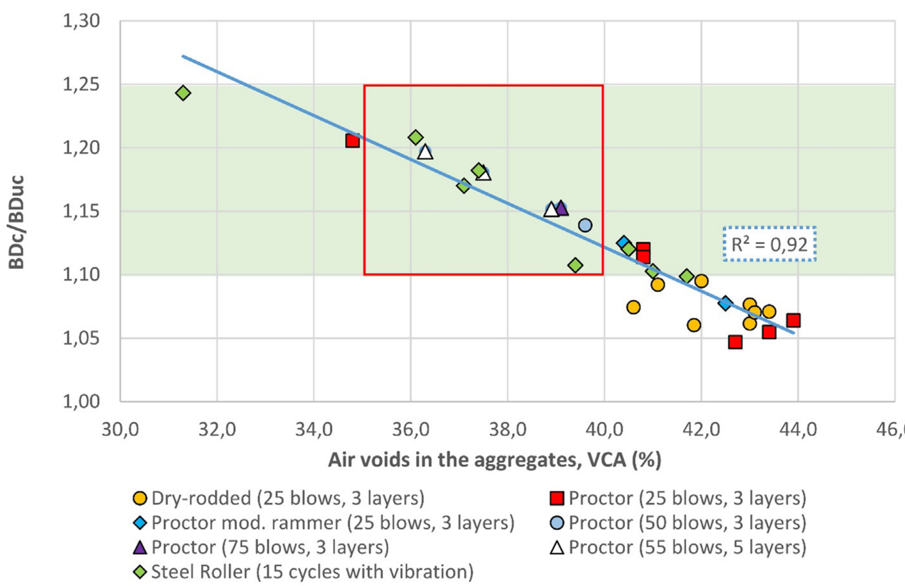

Fig. 8. Relation between air void content and the ratio between compacted & uncompacted aggregates bulk densities.

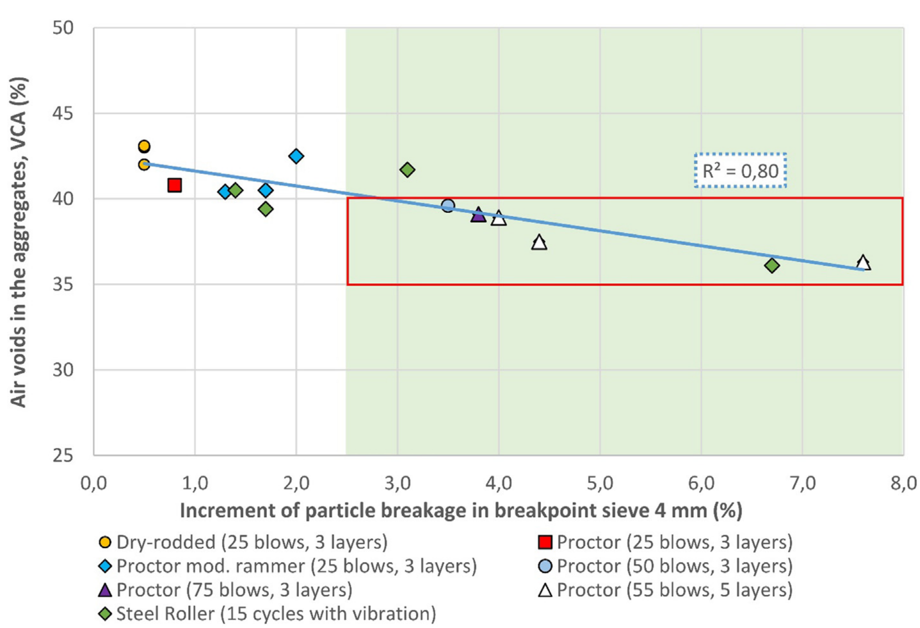

Fig. 9. Relation between air void content and particle breakage in breakpoint sieve.

(1) Laboratory compaction methods using lower energy, such as dry rodded, Proctor (25 blows, 3 layers) and Proctor with modified rammer (25 blows, 3 layers) led to lower particle breakage comparatively to results obtained with asphalt mixtures collected in the field.
(2) VCA showed a satisfactory and good correlation with the particle breakage and the BDc/BDuc ratio, respectively. It was observed that VCA tended to increase with a decrease of the BDc/BDuc ratio.
(3) For the case of SMA 12 and SMA 14, the selected aggregate laboratory compaction method to optimise stone–on-stone effect should have a particle breakage for the breakpoint sieve 4 mm, within the range 2.9% – 8.6% in order to achieve: (i) air void content in the aggregates, between 35% and 40 %, (as reported by [22–23]) to design a SMA with porosity between 2.5% and 5.0%; (ii) BDc/BDuc ratio within 1.10 – 1.25, as specified in Bailey method for SMA mix design, and (iii) to be within the particle breakage values obtained in field SMA.

The results highlight that new laboratory compaction methods described herein, using Proctor (50/75 × 3 layers & 55 blows × 5 layers) and steel roller compactor provide a particle packing more representative of the field conditions comparatively to other methods studied. Further research, focusing on SMA's with other materials applied on the field, is needed in order to recommend one specific method.

Finally, it should be pointed out that the results described in this paper are very significant since a mix design methodology that uses the most adequate compaction methods will produce SMA with improved performance, namely with respect to permanent deformation resistance.

CRediT authorship contribution statement

Henrique Manuel Borges Miranda: Conceptualization, Methodology, Formal analysis, Investigation, Writing - original draft. **Fátima A. Batista:** Resources, Writing - review & editing, Supervision. **Maria Lurdes Antunes:** Resources, Writing - review & editing, Supervision. **José Neves:** Writing - review & editing, Supervision.

Declaration of Competing Interest

The authors declare that they have no known competing financial interests or personal relationships that could have appeared to influence the work reported in this paper.

References

[1] Austroads. Review of Stone Mastic Asphalt design concepts. (Report No. AP–T138/09), Austroads Incorporated, Sidney, Australia, 2009..
[2] EAPA, Long-life asphalt pavements – Technical version, European Asphalt Pavement Association, Breukelen, Netherlands, 2007.
[3] W. Cao, S. Liu, Z. Feng, Comparison of performance of stone matrix asphalt mixtures using basalt and limestone aggregates, Constr. Build. Mater. 41 (2013) 474–479.
[4] E. Iskender, Rutting evaluation of stone mastic asphalt for basalt and basalt–limestone aggregate combinations, Compos. B 54 (2013) 255–264.
[5] E. Allex Alvarez, J.C. Mora, L.V. Espinosa, Quantification of stone-on-stone contact in permeable friction course mixtures based on image analysis, Constr. Build. Mater. 165 (2018) 462–471.
[6] J. Jiang, F. Ni, L. Gao, L. Yao, Effect of the contact structure characteristics on rutting performance in asphalt mixtures using 2D imaging analysis, Constr. Build. Mater. 136 (2017) 426–435.
[7] D. Gardete, L. Picado-Santos, S. Capitão, Improving bituminous mixture performance by optimizing the design compaction energy – A cost effective approach for better pavements, Constr. Build. Mater. 190 (2018) 1173–1181.
[8] E.R. Brown, J.E. Haddock, Method to ensure stone-on-stone contact in SMA paving mixtures. (Report No. 97-02), National Center for Asphalt Technology (NCAT), Alabama, U.S.A., 1997.
[9] W.R. Vavrik, W.J. Pine, G.A. Huber, S.H. Carpenter, R. Bailey, The Bailey method of gradation evaluation: The influence of aggregate gradation and packing characteristics on voids in the mineral aggregate, J. Assoc. Asphalt Paving Technol. 70 (2001) 132–175.
[10] W.R. Vavrik, G. Huber, W.J. Pine, S.H. Carpenter, R. Bailey, Bailey method for gradation selection in hot-mix asphalt mixture design. (Report No. E-C044), Transportation Research Board, Washington, U.S.A., 2002.
[11] P. Polaczyk, B. Huang, X. Shu, H. Gong, Investigation into locking point of asphalt mixtures utilizing Superpave and Marshall compactors, J. Mater. Civil Eng. 31 (9) (2019).
[12] L. Louw, C.J. Semmelink, B.M. Verhaeghe, Development of a stone mastic asphalt design method for South African conditions, Proceedings of the 8th International Conference on Asphalt pavements, 1997.
[13] J. Voskuilen, Ideas for a volumetric mix design method for Stone Mastic Asphalt, Proceedings of the 6th International Conference Durable and Safe Pavements, 2000.
[14] G. Stephenson, F. Bullen, The design, creep and fatigue performance of Stone Mastic Asphalt, in: Proceedings of the 9th International Conference on Asphalt Pavements, Copenhagen, Denmark, 2002..
[15] M.F.C van de Ven, J.L.M. Voskuilen, F. Tolman, The spatial approach of hot mix asphalt, in: Proceedings of the 6th International RILEM Symposium on Performance Testing and Evaluation of Bituminous Materials, Zurich, Switzerland, 2003..
[16] M.M. Jacobs, J.L. Voskuilen, Description of a volumetric type testing and FPC procedure for SMA to prevent premature permanent deformation, In: Proceedings of the International Symposium on Design and Construction of Long Lasting Asphalt Pavements, Alabama, U.S.A., 2004..
[17] Y. Miao, W. Yu, Y. Hou, L. Wang, Investigating the functions of particles in packed aggregate blend using a discrete element method, J. Mater. 12 (2019) 556.
[18] D. Zhang, X.M. Huang, Y.L. Zhao, Aggregate skeleton composition of stone mastic asphalt and its contact properties, J. Jilin Univ. 45 (2) (2015) 394–399.
[19] M. Fakhri, P.T. Kheiry, A.A. Mirghasemi, Modeling of the permanent deformation characteristics of SMA mixtures using discrete element method, Road Mater. Pavement Design 13 (1) (2012) 67–84, https://doi.org/10.1080/14680629.2011.644080.
[20] Austroads, (Report No. AP–T221–13) Sidney, Development of aspects of a design procedure for Stone Mastic Asphalt, Austroads Incorporated, Australia, 2013..
[21] H.M.B. Miranda, F. Batista, M.L. Antunes, J. Neves, A new SMA mix design approach for optimisation of stone-on-stone effect, Road Mater. Pavement Design 20 (2019) 462–479, https://doi.org/10.1080/14680629.2019.1588779.
[22] J.C. Nicholls, E. Loudon, Asphalt surfacings: A guide to asphalt surfacings and treatments used for the surface course road pavements, FN SPON, London, 1998..
[23] L. Drueschner, The German origin of SMA, Australia, Queensland, 2005..
[24] H.M.B. Miranda, Stone Mastic Asphalt – mix design, production, application and performance de Lisboa, Instituto Superior Técnico, Lisbon, Portugal (in Portuguese), 2016..
[25] K. Blazejowski, Stone matrix asphalt: Theory and practice, CRC Press, Taylor & Francis Group, New York, NY, 2011.
[26] W.R. Vavrik, Asphalt mixture design concepts to develop aggregate interlock (Doctoral dissertation), Retrieved from (2000). https://www.ideals.illinois.edu/handle/2142/18830.
[27] L.A. Cooley, E.R. Brown, Potential of using Stone Matrix Asphalt (SMA) for thin overlays. (Report No. 03-01), National Center for Asphalt Technology (NCAT), Alabama, U.S.A, 2003.
[28] R.C. West, R.S. James, Determining Ndesign for SMA mixtures in Alabama. (Report No. 930-584), Alabama Department of Transportation e National Center for Asphalt Technology (NCAT), Alabama, U.S.A., 2005.
[29] R.C. West, J.R. Moore, (Report No. Evaluating Georgia DOT's Compaction Requirements for Stone Matrix Asphalt Mixes 2006 Federal Highway Administration Auburn, U.S.A FHWA-GA-06-203)..